

รายงานวิจัยฉบับสมบูรณ์

โครงการ

การเตรียมและพัฒนาตัวเร่งปฏิกิริยาไบและไตรเมทัลลิกขนาดนาโนด้วยเทคนิคเฟลม สเปรย์ไพโรไลซิสสำหรับปฏิกิริยาดีไฮโดรจิเนชันของโพรเพน

โดย

ผศ. ดร. โอกร เมฆาสุวรรณดำรงและคณะ

สัญญาเลขที่ RMU5380041

รายงานวิจัยฉบับสมบูรณ์

โครงการ

การเตรียมและพัฒนาตัวเร่งปฏิกิริยาไบและไตรเมทัลลิกขนาดนาโนด้วยเทคนิคเฟลมสเปรย์ไพโรไล ซิสสำหรับปฏิกิริยาดีไฮโดรจิเนชันของโพรเพน

ผศ. ดร. โอกร เมฆาสุวรรณดำรง

ภาควิชา วิศวกรรมเคมี คณะวิศวกรรมศาสตร์และเทคโนโลยีอุตสาหกรรม มหาวิทยาลัยศิลปากร

สนับสนุนโดยสำนักงานคณะกรรมการการอุดมศึกษา และสำนักงานกองทุนสนับสนุนการวิจัย

(ความเห็นในรายงานนี้เป็นของผู้วิจัย สกอ.และสกว.ไม่จำเป็นต้องเห็นด้วยเสมอไป)

Abstract

In this research, nanocrystalline tri- and bi-metallic Pt based catalysts have been prepared by conventional impregnation and flame spray pyrolysis methods. Mesoporous material and alumina were used as the catalyst supports. The effect of second and third doping elements on the physiochemical and catalytic properties were also investigated. Physiochemical properties of obtained catalysts were characterized by using X-ray diffraction, nitrogen physisorption, transmission electron microscopy (TEM) combined with energy dispersive X-ray spectroscopy (EDXS), CO chemisorption and X-ray photoelectron spectroscopy (XPS). The catalytic properties of the FSP-made catalysts were investigated in the dehydrogenation of propane. In the case of impregnation-made Pt/MCM-41, Pt-Sn/MCM-41 and Pt-Sn-Ce/MCM-41, it has been found that with suitable amount of tin addition, the platinum dispersion increased. Moreover, the addition of tin could improve propane conversion and propylene selectivity. Also, it could maintain conversion and selectivity about 16 and 87 % respectively. When, the suitable amount of cerium was added, the platinum dispersion also increased. The addition of Ce has little effect on the propylene selectivity but it could obvious improve propane conversion. In the case of FSPmade Pt-Sn and Pt-Sn-X (X=Ce, K, and Zn) supported on Al2O3 catalysts, addition of Ce during FSP synthesis resulted in higher Pt dispersion as well as improved catalytic activity and stability than the non-promoted Pt-Sn/Al2O3. An opposite trend was found with the ones doped with Zn and K in which high surface coverage of Zn and K resulted in a significant loss of Pt active sites. The mechanism for the formation of the trimetallic nanoparticles during one-step FSP synthesis appeared to depend strongly on the differences in the vapor pressure of the metals and the alumina support in flame.

Keywords Flame Spray Pyrolysis, Pt-Sn-Ce/Al₂O₃, Pt-Sn-Ce/MCM-41, dehydrogenation, propane

บทคัดย่อ

ในงานวิจัยนี้ผลึกขนาดนาโนของตัวเร่งปฏิกิริยาแพลทินัมที่มีโลหะผสม 2 ถึง 3 ชนิด ที่ถูก เตรียมขึ้นโดยใช้เทคนิคเคลือบฝั่งแบบแห้งและเฟลมสเปรย์ไพโรไลซิส วัสดุที่มีรูพรุนขนาดกลางและ อะลูมินา๔กนำมาใช้เป็นตัวรองรับ ผลของโลหะตัวที่ 2 และ 3 ที่เติมลงไปต่อสมบัติทางกายภาพและ ความสามารถในการเร่งปฏิกิริยานั้นถูกศึกษา สมบัติทางกายภาพและเคมีของตัวเร่งปกิกิริยาที่ เตรียมขึ้นมาถูกนำไปศึกษาโดยอาศัยเทคนิควิเคราะห์การกระเจิงของรังสีเอ็กซ์ เทคนิคการวัดการ ดูดซับทางกายภาพของแก๊สในโตรเจน กล้องจุลทรรศน์อิเล็กตรอนร่วมด้วยการวัดการกระเจิงของ รังสีเอ็กซ์ เทคนิคการวัดการดูดซับทางเคมีของแก๊สคาร์บอนมอนอกไซด์ และเทคนิคเอ็กซเรย์โฟโต อิเล็กตรอนสเปกโตรสโคปี ความสามารถในการเร่งปฏิกิริยาของตัวเร่งปฏิกิริยาทุกตัวถูกศึกษาใน ปฏิกิริยาดีไฮโดรจิเนชันของโพรเพน ในกรณีของตัวเร่งปฏิกิริยา Pt/MCM-41, Pt-Sn/MCM-41 และ Pt-Sn-Ce/MCM-41 การทดลองพบว่าการเติมดีบุกในปริมาณที่เหมาะสมสามารถเพิ่มความว่องไว และค่าการเลือกเกิดของปฏิกิริยาได้ มันสามารถได้ค่าคอนเวอร์ชันที่ 16 เปอร์เซ็นต์และค่าการเลือก เกิดที่ 87 เปอร์เซ็นต์ตามลำดับ เมื่อซีเรียมถูกเติมในปริมาณที่เหมาะสมค่าการกระจายตัวของโลหะ แพลทินัมจะเพิ่มขึ้น การเติมซีเรียมนั้นส่งผลเพียงเล็กน้อยต่อค่าการเลือกเกิดแต่มันสามารถเพิ่มค่า คอนเวอร์ชันได้ ในกรณีของตัวเร่งปฏิกิริยา Pt-Sn และ Pt-Sn-X (X=Ce, K, and Zn) บนตัว รองรับอะลูมินาที่เตรียมขึ้นโดยใช้เทคนิคเฟลมสเปรย์ไพโรไลซิส การเติมโลหะซีเรียมระหว่าง ขั้นตอนการเตรียมด้วยเทคนิคเฟลมสเปรย์ไพโรไลซิสทำให้กระจายตัวของโลหะแพลทินัมเพิ่มขึ้น เพิ่มความว่องไวและความเสถียรของตัวเร่งปฏิกิริยามากกว่าตัวเร่งปฏิกิริยา Pt-Sn/Al₂O₃ ที่ไม่ได้ ตรงกันข้ามกับการเติมโลหะโปแตลเซียมและสังกะสีซึ่งทากรการกระจายตัว เติมโลหะอื่นลงไป ครอบคลุมพื้นที่จำนวนมากส่งผลให้เกิดการลดลงของกระจายตัวของโลหะแพลทินัมอย่างมาก กลไก ลการเกิดขึ้นของตัวเร่งปฏิกิริยาขนาดนาโนที่มีโลหะ 3 ชนิดในระหว่างการเตรียมโดยใช้เทคนิคเฟ ลมสเปรย์ไพโรไลซิสจะขึ้นกับความแตกต่างของตวามดันไอของโลหะและตัวรองรับอะลูมินาในเปลว ไฟ

คำสำคัญ เฟลมสเปรย์ไพโรไลซิส Pt-Sn-Ce/Al₂O₃, Pt-Sn-Ce/MCM-41ดีไฮโดรจิเนชัน โพ รเพน

Executive Summary

ในงานวิจัยนี้เราได้ทำการศึกษาการเตรียมผลึกขนาดนาโนของตัวเร่งปฏิกิริยา Pt-Sn และ Pt-Sn-X (X=Ce, K, and Zn) บนตัวรองรับอะลูมินา ที่มีปริมาณโลหะแพลทินัม 0.3 เปอร์เซ็นต์โดยน้ำหนัก ปริมาณโลหะดีบุก 1 เปอร์เซ็นต์โดยน้ำหนัก และเติมโลหะตีเรียม โปแต ศเซียมและสังกะสี 0.5 เปอร์เซ็นต์โดยน้ำหนักในขั้นตอนเดียวด้วยเทคนิคเฟลมสเปรย์ไพโรใล ซิส และในงานที่ 2 เราได้ทำการเตรียมผลึกขนาดนาโนของตัวเร่งปฏิกิริยา Pt/MCM-41, Pt-Sn/MCM-41 และ Pt-Sn-Ce/MCM-41 ด้วยเทคนิคการเคลือบฝังแบบแห้ง อนุภาคนาโนที่ เตรียมขึ้นจะถูกนำไปศึกษาหาลักษณะทางเคมีและกายภาพโดยอาศัยเทคนิควิเคราะห์การ กระเจิงของรังสีเอ็กซ์ กล้องจุลทรรศน์อิเล็กตรอนร่วมด้วยการวัดการกระเจิงของรังสีเอ็กซ์ เทคนิคการวัดการดูดซับทาง กายภาพของแก๊สในโตรเจน เทคนิคเอ็กซเรย์โฟโตอิเล็กตรอนสเปกโตรสโคปี นอกจากนี้เรายัง ทดสอบสมบัติในการเป็นตัวเร่งปฏิกิริยาของตัวเร่งปฏิกิริยาที่เตรียมขึ้นทุกตัวด้วยปฏิกิริยาดี ไฮโดรจิเนชันของโพรเพน

ผลที่ได้พบว่าตัวเร่งปฏิกิริยาที่เตรียมจากเทคนิคเฟลมสเปรย์ไพโรไลซิสประกอบไปด้วย อนุภาคผลึกเดี่ยวของแกมมาอะลูมินาซึ่งมีขนาดเของอนุภาคเฉลี่ยอยู่ที่ 7 ถึง 9 นาโนเมตร การ เติมโลหะซีเรียมระหว่างขั้นตอนการเตรียมด้วยเทคนิคเฟลมสเปรย์ไพโรไลซิสทำให้กระจายตัว ของโลหะแพลทินัมเพิ่มขึ้น เพิ่มความว่องไวและความเสถียรของตัวเร่งปฏิกิริยามากกว่าตัวเร่ง ปฏิกิริยา Pt-Sn/Al₂O₃ ที่ไม่ได้เติมโลหะอื่นลงไป ตรงกันข้ามกับการเติมโลหะโปแตสเซียมและ สังกะสีซึ่งทากรการกระจายตัวครอบคลุมพื้นที่จำนวนมากส่งผลให้เกิดการลดลงของกระจายตัวของโลหะแพลทินัมอย่างมาก กลไกลการเกิดขึ้นของตัวเร่งปฏิกิริยาขนาดนาโนที่มีโลหะ 3 ชนิด ในระหว่างการเตรียมโดยใช้เทคนิคเฟลมสเปรย์ไพโรไลซิสจะขึ้นกับความแตกต่างของตวามดัน ไอของโลหะและตัวรองรับอะลูมินาในเปลวไฟ

ในกรณีของตัวเร่งปฏิกิริยา Pt/MCM-41, Pt-Sn/MCM-41 และ Pt-Sn-Ce/MCM-41 การ ทดลองพบว่าการเติมดีบุกในปริมาณที่เหมาะสมสามารถเพิ่มความว่องไวและค่าการเลือกเกิด ของปฏิกิริยาได้ มันสามารถได้ค่าคอนเวอร์ชันที่ 16 เปอร์เซ็นต์และค่าการเลือกเกิดที่ 87 เปอร์เซ็นต์ตามลำดับ เมื่อซีเรียมถูกเติมในปริมาณที่เหมาะสมค่าการกระจายตัวของโลหะ แพลทินัมจะเพิ่มขึ้น การเติมซีเรียมนั้นส่งผลเพียงเล็กน้อยต่อค่าการเลือกเกิดแต่มันสามารถเพิ่ม ค่าคอนเวอร์ชันได้

Chapter I

Introduction

Recently, the catalytic dehydrogenation of propane is becoming more importance because of the growing demand for propylene [¹]. However, the reaction of propane dehydrogenation is an endothermic process that requires a relatively high temperature to obtain a high yield of propylene. Therefore, the deactivation of the catalyst due to coke formation is inevitable because of the reaction conditions. It is important to enhance the propylene yield by developing the catalysts with high-activity, high-stability and high-selectivity [²].

Bimetallic platinum-tin catalysts are widely used in the process of propane dehydrogenation; the Sn promoter of Sn is known to increase the lifetime of Pt-based catalysts by lower due to the reduced the deactivation by coking [³], [⁴], [⁵], [⁶], [⁶] and [⁶]. Larsson et al. [⁶] investigated and pointed out that the bimetallic Pt–Sn catalyst is more resistant to deactivation by coke formation, than the monometallic Pt. Barias et al. [¹⁰] studied Pt and Pt–Sn catalysts supported on α-Al₂O₃ and SiO₂ and found that on α-Al₂O₃ tin interacted with the support and was stabilized in an oxidation state, while on SiO₂ the Sn was more readily reduced and alloy formation was possible. Therefore, the bimetallic Pt–Sn catalyst supported on different carriers can result in the variant interactions between Pt and Sn, which may be affected on the catalytic performance significantly [¹¹]. Among these supports, mesoporous silicate materials such as FSM-16, MCM-41, and SBA-15, which have larger pore diameter and high surface area, have been attracteding wide attention as new materials for catalyst

supports in dehydrogenation reaction [¹²-¹³]. It is expected that this MCM-41 mesoporous support will enhance the performance of the catalyst and reduce the deactivation of catalyst.

Preparation of nanocrystalline materials by aerosol process has received much interest due to high purity of the produced powders, uniformity in chemical composition, narrow size distribution, and regularity in shape. The synthesis of multicomponent materials is easy and readily scale up [14], [15] and [16]. Flame spray pyrolysis (FSP) is one of the aerosol processes that have been applied for preparation of supported metal catalysts in one-step. The characteristics and catalytic properties of FSP-derived catalysts have been investigated in various catalytic reactions including oxidation, hydrogenation, and dehydrogenation [17], [18], [19], [20], [21], [22], [23], [24] and [25]. The flame-made catalysts were often found to exhibit better catalytic performances than the ones prepared by conventional impregnation method. Structural differences between the flame-made and conventionally prepared catalysts have often been explained as the reasons for their differences in the catalytic behaviors.

Rare earth elements, such as lanthanum and cerium, have unique properties which are related to thermal stabilization of alumina support and the strong metal–rare earth oxide interaction [26], [27], and [28]. It has been reported that the main role of CeO₂ in CeO₂/ γ -Al₂O₃ is to improve the thermal stability of the support, which is attributed to the CeAlO₃ formation. Metal–ceria oxide interaction could strongly modify the structural and electronic properties of the supported noble metal [29].

Therefore, the promotion effects of cerium on the catalytic performance of Pt-Sn-Ce/MCM-41 and FSP-made Pt-Sn-Ce/Al₂O₃ catalyst are studied in this research. The purpose of this study was to find the optimum loading of Ce content of the tri-metallic Pt-Sn-Ce/MCM-41 and FSP-made Pt-Sn-Ce/Al₂O₃ for the propane dehydrogenation. The catalyst performance and stability were correlated with their physiochemical properties from various characterization techniques including N₂ physisorption, X-ray diffraction (XRD), CO pulse chemisorption, and transmission electron spectroscopy (TEM).

CHAPTER II

Experimental

2.1 Catalyst Preparations

Preparation of flame-made catalyst

Synthesis of the bi- and tri metallic Pt-Sn/Al₂O₃, Pt-Sn-Ce/Al₂O₃, Pt-Sn-K/Al₂O₃, and Pt-Sn-Zn/Al₂O₃ catalysts was carried out using a spray flame reactor. Platinum actetylacetonate, tin ethylhexanoate, cerium ethylhexanoate, and aluminum butoxide from Aldrich were used as Pt, Sn, Ce, and Al precursors, respectively. Precursors were prepared by dissolving in xylene (MERCK; 99.8 vol.%) with total metal concentration maintained at 0.3 M. The loadings of Pt and Sn were fixed at 0.3 and 1 wt%, respectively. The amount of Ce doping was varied from 0.5 to 1.5wt%. The precursor solution (5 ml/min) of was dispersed into fine droplets by a gas-assist nozzle fed by 5 l/min of oxygen (Thai Industrial Gas Limited; purity >99%) using a syringe pump. The pressure drop at the capillary tip was maintained at 1.5 bar by adjusting the orifice gap area at the nozzle. The spray was ignited by supporting flamelets fed with oxygen (3 l/min) and methane (1.5 l/min) which are positioned in a ring around the nozzle outlet. A sintered metal plate ring (8 mm wide, starting at a radius of 8 mm) provided additional 10 l/min of oxygen as sheath for the supporting flame. The product particles were collected on a glass fiber filter (Whatman GF/C, 15 cm in diameter) with the aid of a vacuum pump.

Preparation of impregnated-made catalyst

Pt/MCM-41 catalysts were prepared by the incipient wetness impregnation of MCM-41 with aqueous solution of Pt precursor (H₂PtCl₆). For Pt-Sn/MCM-41 and Pt-Sn-Ce/MCM-41 catalysts, Sn or Ce was first deposited by impregnation of SnCl₂ ethanol solution and Ce(NO₃)₃ aqueous solution and finally the Pt component was added from aqueous Pt solution in a similar way. In the case of Pt-Sn-Ce/MCM-41 catalysts, Sn or Ce were first deposited by co-impregnation of SnCl₂ and Ce(NO₃)₃ ethanol solution and finally the Pt component was added as described previously. After that the catalysts were calcined at 500°C for 4 h, and then dechlorinated at 500°C for 4 h in air containing steam and finally reduced under H₂ at 500°C for 1 h.

To compare the activity of flame-made catalyst, the bi-and tri-metallic catalysts were prepared by incipient wetness impregnation, using organic solutions of platinum actetylacetonate, tin ethylhexanoate, and cerium 2ethylhexanoate in xylene. The incipient wetness impregnation procedure is as follow:

- The PtSnCe catalyst was prepared by co-impregnation. The metal contents in the catalysts were 0.3wt% for Pt, 1wt% for Sn, and 0.5-1.5wt% Ce. A commercial (JRC-AlO2) and flame-made Al₂O₃ were used as the catalyst support.
- 2) Both aluminas were impregnated with the droplet of metal solution.
- 3) The obtained powder was dried in air at 110°C overnight and then calcined at 550°C in air for 3 hour

2.2 Catalyst Characterization

To investigate the physiochemical properties of catalysts, fresh and spent catalysts was characterized by several techniques

1. N_2 -physisorption

The BET (Brunauer Emmett Teller) surface area, average pore size diameters, and pore size distribution are obtained from nitrogen adsorption/desorption isotherms determined at liquid nitrogen temperature on an automatic analyzer using Micromeritics ASAP 2020 (surface area and porosity analyzer).

2. X-ray Diffraction (XRD)

The bulk crystal structure and chemical phase composition are determined by diffraction of an X-ray beam as a function of the angle of the incident beam. The XRD spectrum of the catalyst is measured by using a SIEMENS D500 X-ray diffractometer and $Cu\ K_{\alpha}$ radiation. The crystallite size is calculated from Scherrer's equation.

3. Transmission Electron Microscopy (TEM)

The morphology, particle size and particle distribution will be observed using JEOL-JEM 200CX transmission electron microscope operated at 100 kV.

4. CO-pulse chemisorptions

The active sites and relative percentages dispersion of platinum catalyst were determined by CO-pulse chemisorption technique using a Micromeritics ChemiSorb 2750 system attached with ChemiSoft TPx software at room temperature.

5. X-ray Photoelectron Spectroscopy (XPS)

XPS analysis was performed using an AMICUS photoelectron spectrometer equipped with a Mg K_{α} X-ray as a primary excitation and a KRATOS VISION2 software. XPS elemental spectra were acquired with 0.1 eV energy step at a pass energy of 75 kV. The C 1s line was taken as an internal standard at 285.0 eV.

6. Thermal Gravimetric and Differential Temperature Analysis (TG/DTA)

Amount of coke deposited on the surface of catalyst were detected by Thermal gravimetric and differential temperature analysis (TG/DTA) using an SDT Analyzer Model Q600 from TA Instruments, USA

2.3 Catalytic Evaluation

The dehydrogenation of propane (Thai Industrial Gas) was carried out in a fixed-bed reactor with an inner diameter 6 mm. Approximately 0.1 g of catalyst was loaded in the middle of reactor. Prior to the experiments the catalysts were pretreated in flowing H_2 (30 ml/min) at 773 K for 1 h. The reaction was carried out isothermally at 823 K and at atmospheric pressure. The reaction mixture composed of H_2 , C_3H_8 and $H_2/C_3H_8/A$ r molar ratio = 1:1:5) was fed to the reactor with the weight hourly space velocity (WHSV) based on propane of 5 h⁻¹. A purge gas (Ar) flow of 30 ml/min was used and the reaction mixture was preheated at 773 K. The product gases

were analyzed on-line using a gas chromatograph with a TCD detector using SUS Column PorapakQ, 80/100 mesh column.

CHAPTER 3

Results and Discussion

3.1 Effect of promoters (Ce, Zn and K)

3.1.1 Catalyst properties

Figure 1 shows the XRD patterns of flame-made Pt-Sn/Al₂O₃ and Pt-Sn-X/Al₂O₃ (X = Ce, Zn and K) catalysts. All the catalyst samples exhibited only the characteristic peaks of γ -Al₂O₃ with no additional peaks corresponding to Pt, Sn, Ce, Zn, K and other alumina phases. This probably due to the low amount of Pt, Sn and the third doping element loading and/or high dispersion of these metals on the Al₂O₃ supports. It is also indicated that additional of Pt, Sn or other doping elements simultaneously with Al during flame synthesis did not affect alumina phase composition.

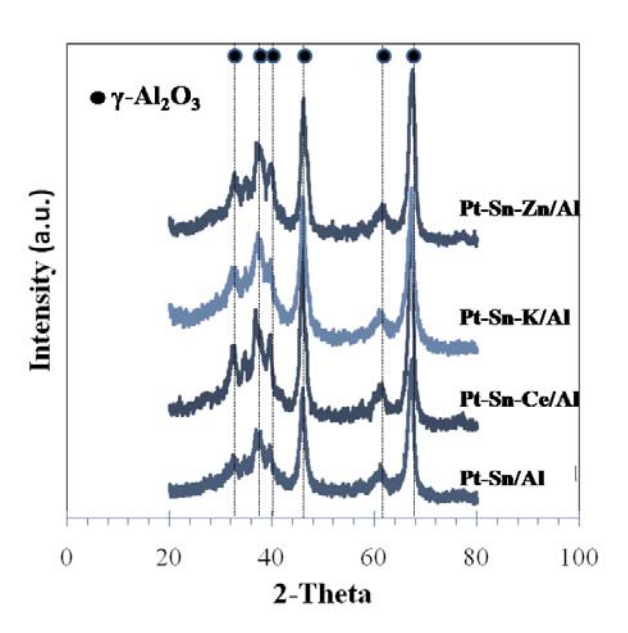


Figure 1 The XRD patterns of flame-made $Pt-Sn/Al_2O_3$ and $Pt-Sn-X/Al_2O_3$ (X = Ce, Zn and K) catalysts (as synthesized)

TEM micrographs of the flame-made Pt-Sn/Al₂O₃ and Pt-Sn-X/Al₂O₃ (X = Ce, Zn and K) catalysts are illustrated in **Figure 2**. All the flame-made powder consisted of spherical primary particles with the size around 5 to 20 nm. Small metal particles/clusters with the average size around 4-9 nm were observed for Pt-Sn-K/Al₂O₃ and Pt-Sn-Zn/Al₂O₃ catalysts as dark spots, while they were not distinguishable for the unloaded and Ce-loaded catalysts. Such results suggest that loading with K and Zn increased the metal cluster size of Pt-Sn/Al₂O₃ catalysts.

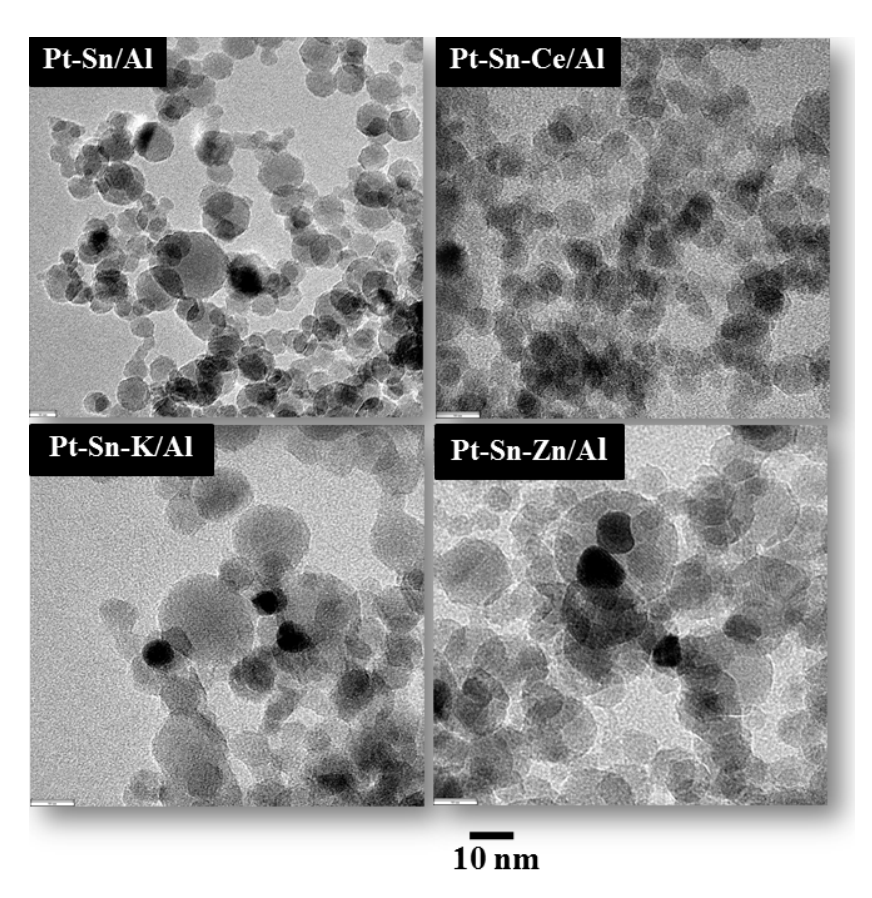


Figure 2 The TEM micrographs of flame-made $Pt-Sn/Al_2O_3$ and $Pt-Sn-X/Al_2O_3$ (X = Ce, Zn and K) catalysts

Table 1 summarizes physicochemical properties of the flame-made Pt- Sn/Al_2O_3 and Pt-Sn-X/Al₂O₃ (X = Ce, Zn and K) catalysts. The crystallite size of all catalysts was ranged between 7 to 9 nm which was in good agreement with the particle size measured from TEM images, indicating that the particles were single crystalline. The BET surface areas of all flame-made catalysts were ranged between 89 and 153 m²/g. A huge increase in BET surface area of the flame-made Pt-Sn-K/Al₂O₃ catalysts corresponding to the smallest crystallites size compared to the other flame-made catalysts was due probably to inhibition of the growth of the Al₂O₃ particles by K dopant. From N₂ adsorption results (Figure 3), all doping catalysts were nonporous with macro-pore structure. The same structure had been reported for flame-made Al₂O₃, Pt/Al₂O₃ and Pt-Sn/Al₂O₃ in our earlier works [20]. The relative amounts of active surface Pt metal on the catalyst samples were calculated from CO chemisorption. The calculation of Pt active sites was based on the assumption that one carbon monoxide molecule adsorbs on one platinum site. The Pt active sites were found to increase from 1.22x10¹⁸ to 4.25x10¹⁸ sites/g-catalyst after loading with 0.5 wt% of Ce corresponding to increasing of %Pt metal dispersion from 14.6 to 49.5%. On the other hand, doping the Pt-Sn/Al₂O₃ catalysts with K and Zn during FSP synthesis resulted in significant loss of the Pt active sites. The amounts of CO chemisorption were negligible on the Pt-Sn-K/Al₂O₃ and Pt-Sn-Zn/Al₂O₃ catalysts. It has been suggested by Vu et al. [30] that incorporation of Ce in Al₂O₃ lattice during the preparation of mesoporous alumina can improve metal dispersion of Pt-Sn/Al₂O₃ catalysts.

Surface compositions in term of M/Al (M = Sn, Ce, K, Zn) atomic ratio of the various FSP-made Pt-Sn/Al₂O₃ and Pt-Sn-M/Al₂O₃ catalysts were determined by XPS

technique and the results are given in **Table 1**. Sn/Al ratios of all samples were quite constant in a range of 0.005-0.008. It should be noted that K/Al and Zn/Al atomic ratio for Pt-Sn-K/Al₂O₃ and Pt-Sn-Zn catalyst were more than ten times higher than the Sn/Al atomic ratios, indicating that both K and Zn atoms were highly dispersed on the catalyst surface. While the Ce/Al atomic ratio for Pt-Sn-Ce/Al₂O₃ was not much different from its Sn/Al atomic ratio. Thus, coverage of K and Zn molecule on the catalyst surface could be the reason for the drastically decrease of Pt metal active sites measured by CO chemisoprtion technique and increase of metal cluster size. Different of dopant dispersion on catalyst surface can be explained by the formation process during FSP as follows: first the sprayed droplets of precursor solution were evaporated and combusted as soon as they met the flame and released the metal atoms; then nucleation and growth of particles by coagulation and condensation occurred along the axial direction of the flame. Since the vapor pressure of Al₂O₃ was lower than those of the metals, the formation of Al₂O₃ particles could start earlier. Further downstream of the flame at lower temperature, Pt and other dopants started to form small particles and/or deposits directly on the Al₂O₃ support. In the case of K and Zn dopant, the boiling points of those two metals were much lower than Pt and Sn which resulted in late formation and deposition on Pt and Sn surface. For Pt-Sn-Ce/Al₂O₃ catalyst, Pt and Ce could be formed simultaneously due to their similar boiling point. Moreover, addition of Ce could inhibit the growth of Pt cluster resulting in an increase of Pt active sites.

 $\textbf{Table 1} \ Physicochemical \ Properties \ of \ Flame-made \ Pt-Sn/Al_2O_3 \ and \ Pt-Sn-X/Al_2O_3 \ (X=Ce, \ Zn \ and \ K) \ Catalysts$

Catalyst	Crystallite size (nm)	BET Surface Areas (m²/g)	CO Chemisorption Results			XPS results			
			CO uptake (molecule CO/g cat.)	%Pt dispersion	d _P Pt ⁰ (nm)	Sn/Al	Ce/Al	K/Al	Zn/Al
Pt-Sn/Al ₂ O ₃	9	112	$1.22 x 10^{18}$	14.6	7.4	0.005	-	-	-
Pt-Sn-Ce/Al ₂ O ₃	8	95	4.25×10^{18}	45.9	2.4	0.005	0.007	-	-
$Pt-Sn-K/Al_2O_3$	7	153	n.d.	n.d.	n.d.	0.006	-	0.097	-
$Pt-Sn-Zn/Al_2O_3$	9	100	n.d.	n.d.	n.d.	0.008	-	-	0.092

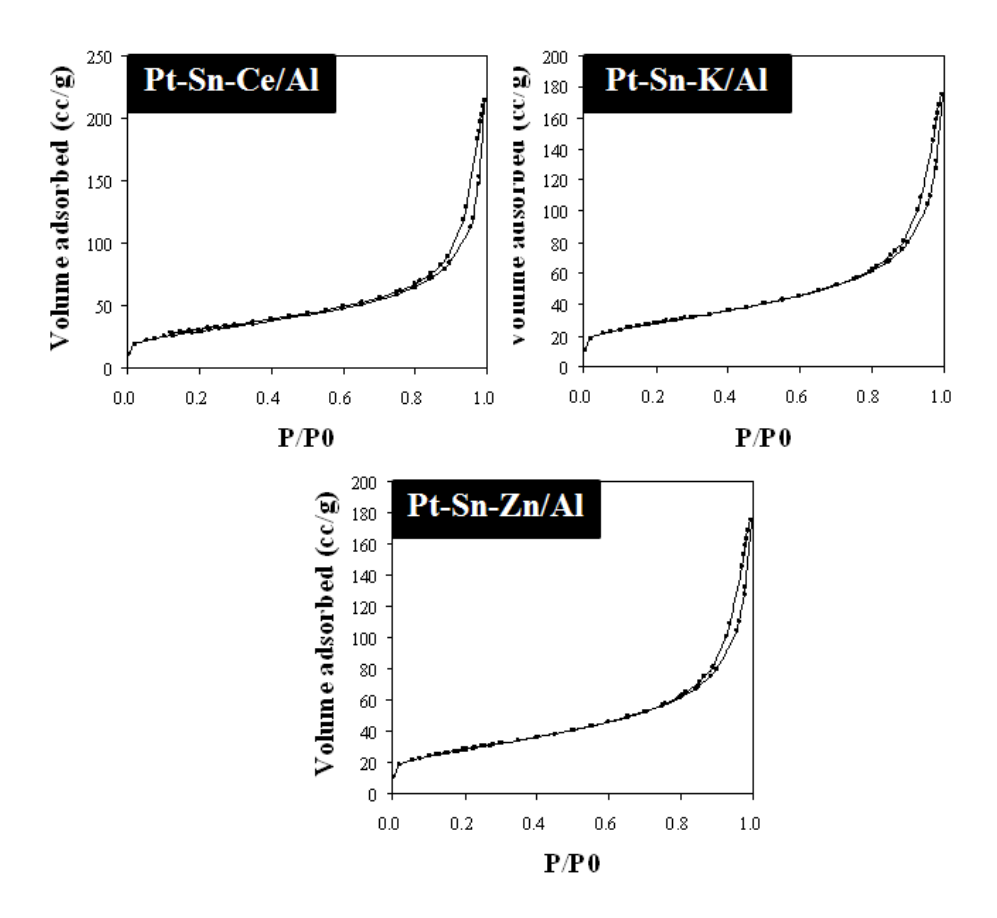


Figure 3 N_2 adsorption isotherms of Pt-Sn-X/Al₂O₃ (X = Ce, Zn and K) catalysts

3.1.2 Dehydrogenation of propane

The catalytic behavior of the flame-made Pt-Sn/Al $_2$ O $_3$ and Pt-Sn-X/Al $_2$ O $_3$ (Ce, Zn and K) catalysts was investigated in the dehydrogenation of propane reaction. The catalytic performance in terms of propane conversions and selectivity to propene of the flame-made Pt-Sn/Al $_2$ O $_3$ and Pt-Sn-X/Al $_2$ O $_3$ (Ce, Zn and K) catalysts are summarized in **Table 2**. The conversion of propane for the flame-made catalysts was improved in order of Pt-Sn-Ce/Al $_2$ O $_3$ > Pt-Sn/Al $_2$ O $_3$ > Pt-Sn-Zn/Al $_2$ O $_3$ > Pt-Sn-K/Al $_2$ O $_3$ and Pt-Sn-Ce/Al $_2$ O $_3$ was in the range of 96 to 97% while the selectivity of Pt-Sn-K/Al $_2$ O $_3$ and Pt-Sn-Zn/Al $_2$ O $_3$ decreased to 70% and 76%, respectively. The better catalytic performance of the

flame-made Pt-Sn-Ce/ Al_2O_3 catalysts was correlated well with an increase of Pt dispersion during FSP synthesis.

Table 2 Catalytic Properties for propane dehydrogenation

Catalyst	% Con	version	%C ₃ H ₆ selectivity		
		Final ^b	-		
Pt-Sn/Al ₂ O ₃	29.1	17.8	97		
Pt-Sn-Ce/Al ₂ O ₃	45.3	38.6	95		
$Pt-Sn-K/Al_2O_3$	4.5	4.1	70		
$Pt\text{-}Sn\text{-}Zn/Al_2O_3$	8.6	8.1	76		

^a 15 min

^b 120 min

3.2 Effect of Ce doping content

3.2.1 Catalyst Characteristics

Figure 4 shows the XRD patterns of the flame-made Pt-Sn and Pt-Sn-Ce catalysts with Ce loading 0.5, 1.0 and 1.5 wt%. The characteristic peaks of pure gamma phase alumina were observed with small contamination of alpha-alumina for all the samples. The XRD characteristic peaks corresponding to platinum, tin and cerium species were not detected for all the catalysts due to low amount of metals present and/or high dispersion of these metals on the Al₂O₃ supports. The addition of Pt, Sn, and Ce during flame synthesis of Al₂O₃ particles did not affect the alumina phase composition.

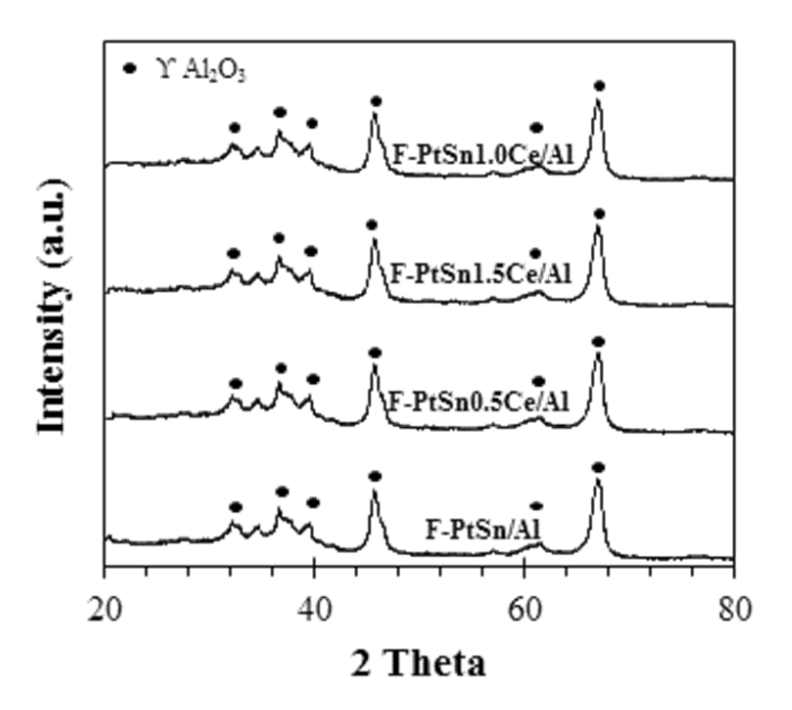


Figure 4 XRD patterns of the flame-made Pt-Sn-Ce/Al₂O₃ catalysts (as-synthesized)

Table 3 summarizes physicochemical properties of the flame- and impregnation-made catalysts. The crystallite size of all catalysts was ranged between 8 to 10 nm which was in good agreement with the particle size measured from TEM images (Figure 5), indicating that the particles were single crystalline. From the TEM micrographs, Pt/PtO metal clusters were not distinguishable in all the flame-made samples due probably to poor contrast between the Pt and Al atoms. The BET surface areas of flame-made Pt and Pt-Sn/Al $_2$ O $_3$ catalysts were 110 and 112 m^2/g , respectively. The BET surface area decreased from 112 to $83 \text{ m}^2/\text{g}$ as the Ce content increased from 0 to 1.5wt%. Decreasing in BET surface area could be attributed to pore blockages by metal/metal oxide clusters. Average pore diameter and pore volume are also reported in **Table 3**. All flame-made catalysts had the similar average pore diameter around 9 to 12 nm and the pore volume around 19 to 21 cm³/g. The FSP-made catalysts exhibited the hysteresis loop of type A and gave rise of hysteresis at relatively high partial pressure (not shown here), which indicated the formation of opened cylindrical pore structure and contained only large interparticle pores (macropore) as suggested in our earlier works.

 $\textbf{Table 3} \ Physicochemical \ Properties \ of \ Flame- \ and \ impregnation-made \ Al_2O_3 \ and \ Pt-Sn/Al_2O_3 \ Catalysts$

Catalyst	Crystallite size (nm)	BET Surface Areas (m²/g)	Average Pore Diameter (nm)	Pore Volume (cm3 (STP)/g)	CO Chemisorption Results		
				-	CO uptake (molecule	%Pt	d _P Pt ⁰
					CO/g cat.)	dispersion	(nm)
F-Pt/Al ₂ O ₃	8	110	10	22	2.32×10^{18}	28	3.9
$F-Pt-Sn/Al_2O_3$	8	112	9	20	$1.22 x 10^{18}$	14.6	7.4
F-Pt-1Ce/Al ₂ O ₃	9	93	10	21	5.85×10^{18}	63.2	1.7
F-Pt-Sn-0.5Ce/Al ₂ O ₃	8	95	11	19	4.25×10^{18}	45.9	2.4
F-Pt-Sn-1Ce/Al ₂ O ₃	8	85	8	20	$5.13x10^{18}$	55.5	1.9
F-Pt-Sn-1.5Ce/Al ₂ O ₃	10	83	12	19	$1.77 x 10^{18}$	19.2	5.6
I-Pt-Sn-1Ce/F-Al ₂ O ₃	9	90	10	22	4.36×10^{18}	47.1	2.3
I-Pt-Sn-1Ce/RefAl ₂ O ₃	6	147	6	33	4.18×10^{18}	45.1	2.4

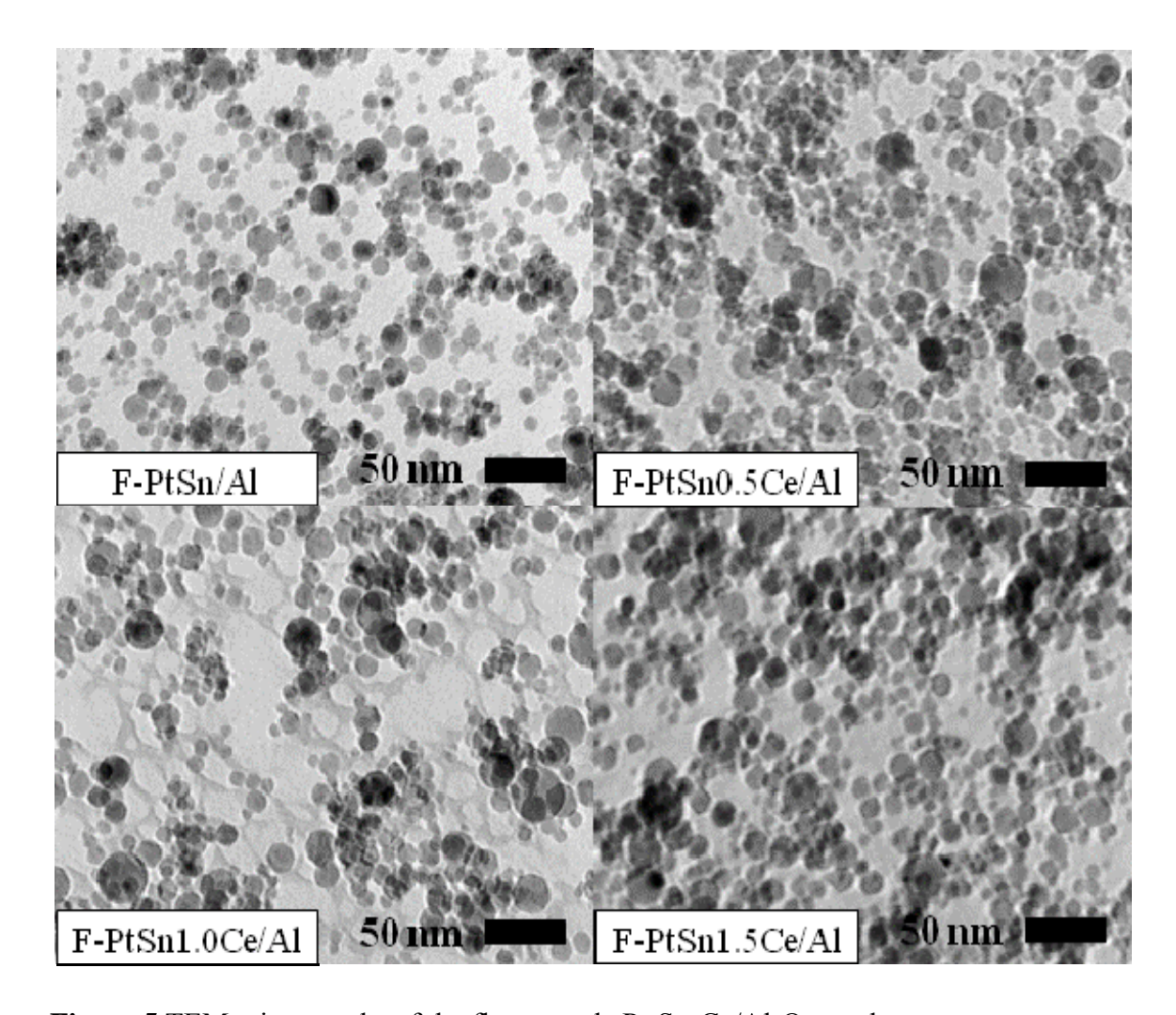


Figure 5 TEM micrographs of the flame-made Pt-Sn-Ce/Al₂O₃ catalysts

The relative amounts of active surface Pt metal on the catalyst samples were calculated from CO chemisorption based on the assumption that one carbon monoxide molecule adsorbs on one platinum site. For bimetallic Pt-based catalyst, addition of 1wt% Sn resulted on the decreasing of Pt active site from 2.32x10¹⁸ to 1.22x10¹⁸ sites/g-catalyst, whereas, the Pt active site increased to 5.85x10¹⁸ sites/g-catalyst after loading with 1wt%Ce. The lower amount of CO chemisorption on the Pt–Sn catalysts can be attributed to the formation of Pt–Sn ensembles or alloys that do not adsorb CO or the formation of an alumina matrix (i.e., in the form of Al–O groups) covering the Pt and Sn surfaces during FSP synthesis. In the case of Pt-Ce catalysts, the

improvement of Pt dispersion by addition of Ce has been explained by Vu et al. [31]. They suggested that the incorporation of Ce in Al₂O₃ lattice during the preparation of the catalyst can improve Pt metal active sites and dispersion of Pt-Sn/Al₂O₃ catalysts. In our case, the preparation of the catalyst took place in the gas phase which the Pt and Ce could be formed simultaneously and the addition of Ce inhibited the growth of Pt cluster resulting in an increasing of Pt active sites. In the case of tri-metallic Pt-Sn-Ce catalysts, the Pt active sites were found to increase from 1.22x10¹⁸ to 5.13x10¹⁸ sites/g-catalyst when Ce loading increased from 0 to 1 wt% corresponding to the increasing of %Pt metal dispersion from 14.6 to 55.5%. However, further increasing of Ce loading content to 1.5 wt%, the Pt active sites and metal dispersion decreased to 1.77x10¹⁸ and 19.2%, respectively. This result indicates that with the excessive Ce doping amounts, the ceria species may block the platinum surface, hence the dispersion of platinum decreased.

Figure 6 presents the TPR profiles of flame-made Pt, Pt-Sn and Pt-Sn-Ce supported on alumina catalysts. The TPR profiles of flame-made Pt/Al₂O₃ showed two reduction peaks at 300°C and 513°C, suggesting two types of platinum species with differences in the interaction between Pt species and the Al₂O₃ support. First peak can be assigned to a weak interaction with the support and the other in a strong interaction with the support [³²-³³]. In the case of flame-made Pt-Sn/Al₂O₃ catalysts, the reduction peaks in the TPR profiles shifted to lower reduction temperatures, one at 245°C, and the other at 498°C comparable to that in the TPR profiles of Pt/Al₂O₃. The amount of H₂ consumed at low temperature increased due to the reduction of SnO₂ occurs concurrently at low temperature to form PtSn alloy [³⁴]. The Pt-Sn-Ce/Al₂O₃ exhibited two broad reduction peaks at 200 to 400 °C and 478°C. The broad reduction

peaks indicate the strong interactions between the three components (Pt, Sn and Ce). The shift to lower reduction temperature of second peak would be explained by the Pt-Ce interaction leading to the easier reduction of ceria by hydrogen spillover from Pt to cerium oxide [35_36].

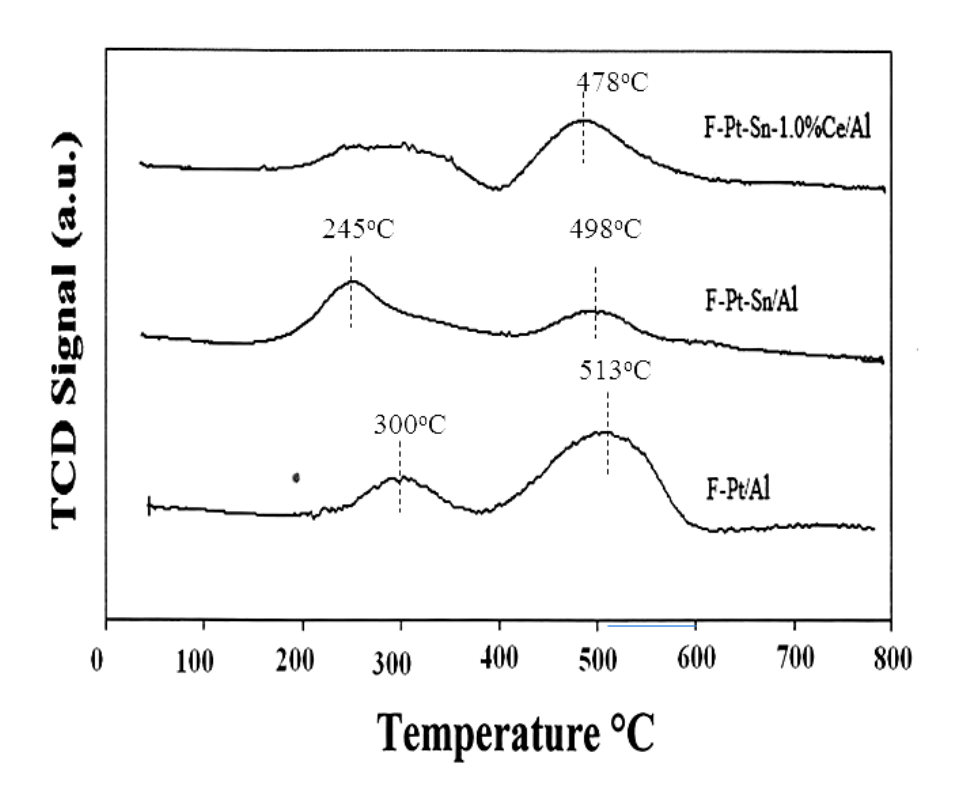


Figure 6 TPR profiles of flame-made Pt, Pt-Sn, and Pt-Sn-Ce supported on alumina catalysts.

3.2 Propane dehydrogenation results

The effect of Ce loading on the catalytic performance of the flame-made Pt-Ce/Al₂O₃ and Pt-Sn-Ce/Al₂O₃ catalysts was investigated in the dehydrogenation of propane reaction at 823 K. The catalytic performances in terms of propane conversion, selectivity to propylene, and catalyst stability are shown in **Table 4**. The impregnation-made Pt-Sn-Ce supported on flame-made and reference Al₂O₃ supports were used for comparison purposes. The conversion of propane for the flame-made

Pt/Al₂O₃ and Pt-Sn/Al₂O₃ exhibited much higher propane conversion, compared to the mono- and bimetallic Pt-Sn. The conversion of propane increased to 38.6 and 49.7% for Ce loading 0.5 and 1 wt%, respectively. However, further increase of Ce loading to 1.5 wt% did not result in additional improvement of the catalyst activity (propane conversion 48.3%). Comparing the FSP-made bimetallic catalysts, propane conversion of Pt-Ce/Al₂O₃ was twice higher than that of Pt-Sn/Al₂O₃, which could be attributed to the higher Pt dispersion.

Table 4 Results of propane dehydrogenation^a

Catalyst	% Conversion ^b		%C ₃ H ₆ selectivity	%Deactivation ^c	
-	Initial	Final	_		
F-Pt/Al ₂ O ₃	11.8	7.3	97	38	
$F-Pt-Sn/Al_2O_3$	29.1	19.8	97	31	
F-Pt-1Ce/Al ₂ O ₃	42.7	36.5	95	15	
F-Pt-Sn-0.5Ce/Al ₂ O ₃	45.3	38.6	95	15	
F-Pt-Sn-1Ce/Al ₂ O ₃	56.5	49.7	95	12	
F-Pt-Sn-1.5Ce/Al ₂ O ₃	51.2	48.3	93	6	
I-Pt-Sn-1Ce/F-Al ₂ O ₃	42.4	37.1	92	13	
I-Pt-Sn-1Ce/RefAl ₂ O ₃	42.6	37.2	91	13	

^aThe reaction conditions were 823 K at atmospheric pressure, $H_2/C_3H_8/Ar$ molar ratio = 1:1:5 and WHSV = 5 h⁻¹

^bAfter 15 min and 180 min

^{co}%Deactivation = (Initial conversion – Final conversion)/Initial conversion × 100

For similar Ce content (1 wt% loading), the FSP-made Pt-Sn-Ce/Al₂O₃ catalysts exhibited higher propane conversion than the impregnation-made ones (propane conversion 37.1%). There were no significant differences between the impregnation-made catalysts supported on the FSP- and reference Al₂O₃.

The plots of propane conversion versus reaction time are shown in **Figure 7**. The conversion of propane gradually decreased during the 180 min time-on-stream, suggesting catalyst deactivation due probably to coke formation [37]. The percentages of catalyst activity change are summarized in **Table 4**. The deactivation rate decreased when Sn and Ce were added to the Pt/Al₂O₃ catalysts. The percent deactivation decreased from 38 to 31 and 15% for the catalysts doped with 1 wt% Sn and 1 wt% Ce, respectively. In the case of Pt-Sn/Al₂O₃, addition of 1.5 wt% Ce resulted in the reducing of percent deactivation from 31 to 6%. There was no significant difference in terms of propylene selectivity for all the catalysts (propylene selectivity \approx 91-97%).

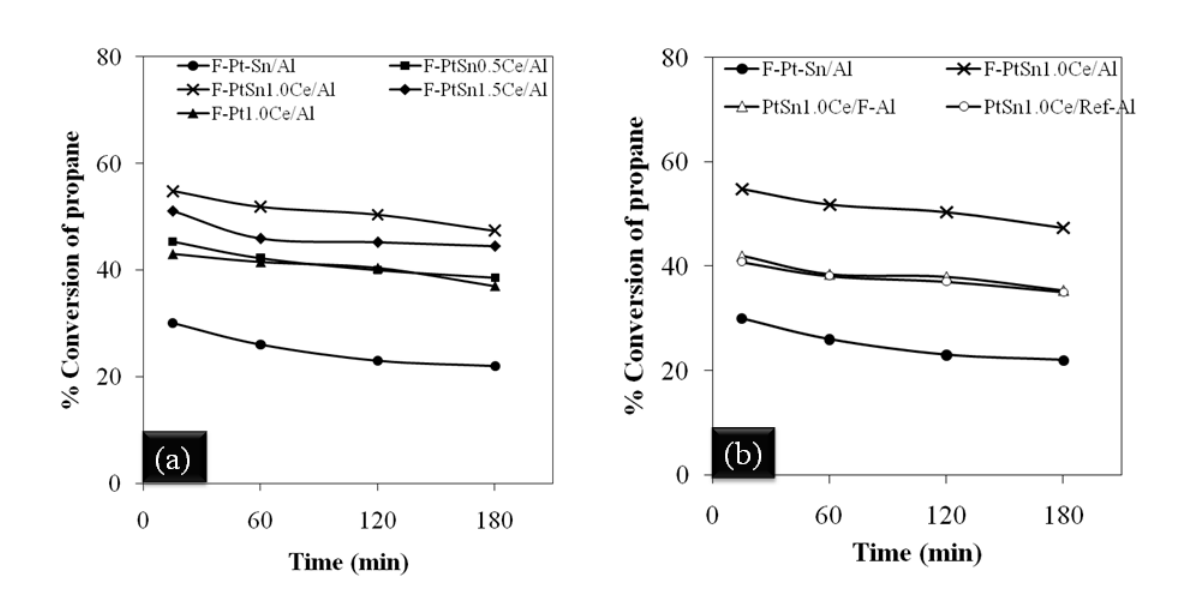


Figure 7 Plot between propane conversion and reaction time of all the catalysts

3.3 Effect of Ce addition on Pt-Sn/MCM-41 catalyst

3.3.1 Physiochemical properties

Figure 8 shows the XRD patterns of all the catalyst samples. The powder exhibited the XRD pattern of mesoporous structure of MCM-41 without any contamination phases of Pt, Sn, or Ce (not shown here). This suggests that the amounts of deposited metal/metal oxide on the MCM-41 surface were small and/or they were highly dispersed. As can be seen, the XRD patterns between Pt/MCM-41 and different catalysts were very similar, indicating that the original structure of the MCM-41 was not destroyed during the process of impregnation and calcination.

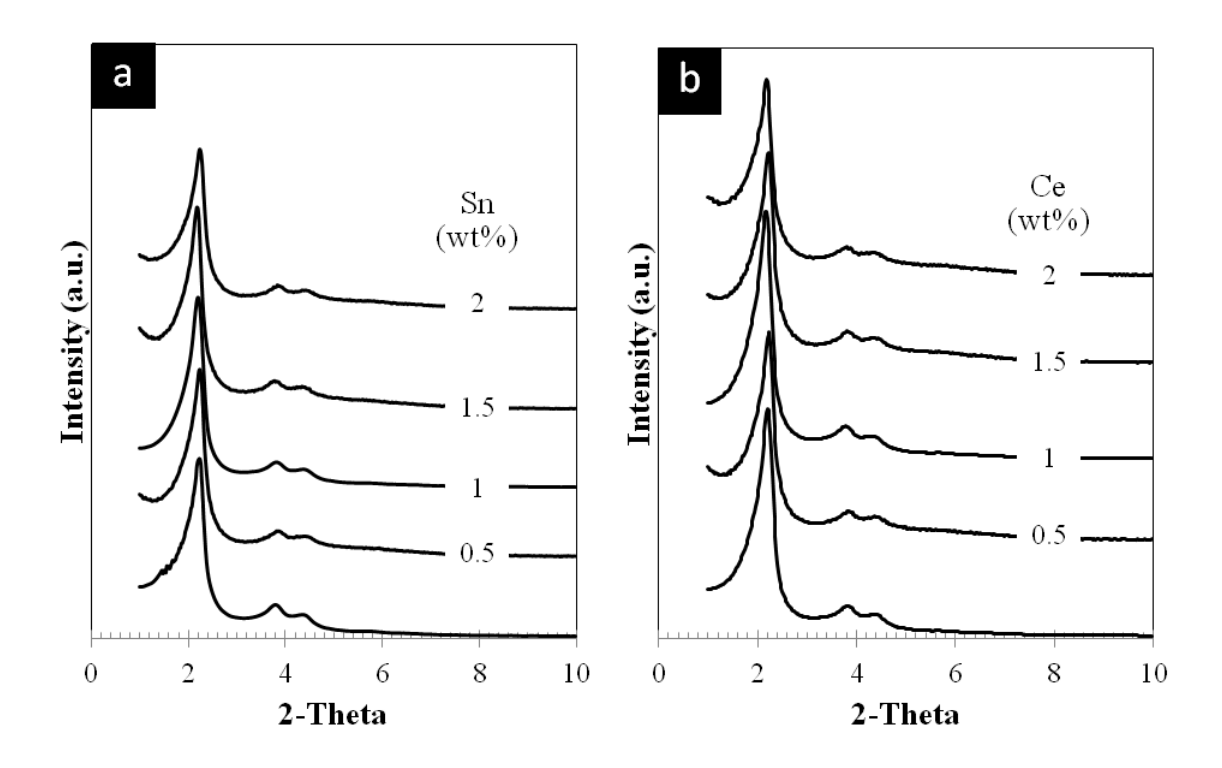


Figure 8 XRD patterns of all catalyst samples

The BET surface areas, total pore volumes, and average pore diameter of MCM-41, Pt/MCM-41, Pt-Sn/MCM-41 with different Sn loadings and Pt-Sn-Ce/MCM-41 with different Ce loadings are summarized in **Table 5**. It is apparent that MCM-41 materials possessed the largest BET surface area. There was a slight change in BET surface area and pore volume after Sn and Ce loading, suggesting that some Sn and Ce species entered into the channels of MCM-41. The nitrogen adsorption-desorption isotherms of the catalysts are presented in **Figure 9**. All the catalysts showed the adsorption-desorption isotherm correspond to the type IV isotherm. The addition of Sn and Ce did not obviously change the average pore diameter of the MCM-41.

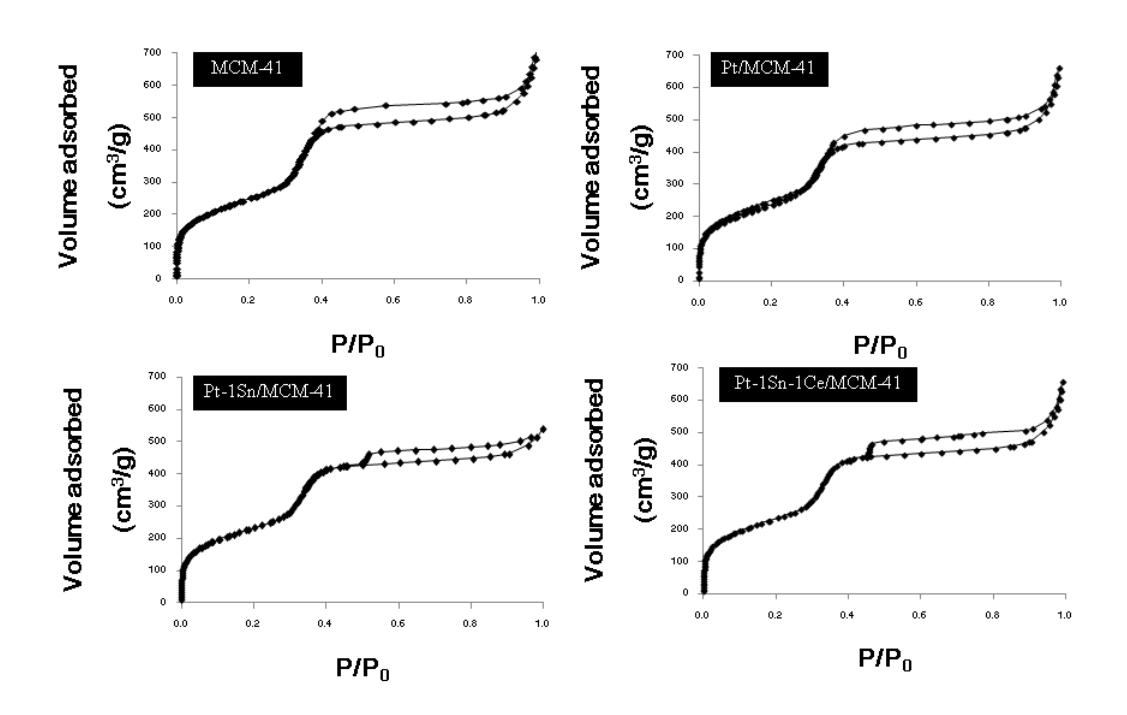


Figure 9 The nitrogen adsorption-desorption isotherms of the catalysts

 Table 5 Physicochemical Properties of Pt, Pt-Sn and Pt-Sn-Ce supported on MCM-41 catalysts

Catalyst	BET Surface Areas (m²/g)	Average Pore Diameter (nm)	Pore Volume (cm ³ (STP)/g)	CO Chemisorption Results		
			_	CO uptake (molecule	%Pt	d _P Pt ⁰
				CO/g cat.)	dispersion	(nm)
MCM-41	1,280	1.1	3.3	-	-	-
Pt/MCM-41	1,196	1.0	3.3	2.8×10^{18}	17.9	10.0
Pt-Sn(0.5%)/MCM-41	1,206	1.0	3.3	5.1 x 10 ¹⁸	33.3	5.4
Pt-Sn(1.0%)/MCM-41	1,146	0.8	2.9	6.6 x 10 ¹⁸	42.7	4.2
Pt-Sn(1.5%)/MCM-41	1,134	0.8	2.9	6.1 x 10 ¹⁸	39.7	4.5
Pt-Sn(2.0%)/MCM-41	1,096	0.9	3.4	3.4×10^{18}	22.0	8.2
Pt-Sn-Ce(0.5%)/MCM-41	1,182	1.0	3.4	7.7 x 10 ¹⁸	49.9	3.6
Pt-Sn-Ce(1.0%)/MCM-41	1,193	1.0	3.4	8.7 x 10 ¹⁸	56.6	3.2
Pt-Sn-Ce(1.5%)/MCM-41	1,087	0.9	3.4	8.2 x 10 ¹⁸	53.2	3.4
Pt-Sn-Ce(2.0%)/MCM-41	1,154	1.0	3.4	8.0 x 10 ¹⁸	51.8	3.5

The amounts of actives sites and dispersion of Pt on MCM-41 supports were measured by CO pulse chemisorption. The calculation of Pt active sites is based on the assumption that one molecule of carbon monoxide adsorbs on one platinum site. The results are also given in **Table 5**. It can be seen that, the metal dispersion increased from 33.28 to 42.67 % with increasing of Sn loading contents from 0.5 to 1.0 wt%. However, the Pt metal dispersion decreased to 39.7 and 22% with further increasing of Sn loading to 1.5 and 2.0 wt%, respectively. When the concentration of Sn was excessive, it may block the platinum particles, which caused the decrease of the CO chemisorption sites. The presence of cerium can also affect the platinum dispersion. Compared to the Pt-Sn(1.0 wt%)/MCM-41 catalyst, suitable amount of Ce addition resulted in an obvious increase of the metal dispersion. However, with the excessive addition of Ce (1.5 wt%), opposite trend was observed. It has been reported that suitable content of base-metal oxide additives can protect the agglomeration of dispersed Pt, resulting in an increase in platinum dispersion. Nevertheless, when the excessive concentration of Ce was added, amounts of cerium block the platinum particles, lowering the metal dispersion instead.

The TEM micrographs of the Pt/MCM-41, Pt-Sn/MCM-41 and Pt-Sn-Ce/MCM-41catalysts are shown in **Figure 10**. The typical shapes of the Pt/PtO particles were nearly spherical. The particle sizes of Pt/PtO deposited on MCM-41 were around 16 – 18 nm. The Pt-Sn (loading 0.5, 1.0 and 2.0 wt%)/MCM-41 consisted of Pt/PtO particles with average size between 2-4 nm. The size distribution of metallic particles over Pt-Sn(0.5 wt%)/MCM-41 and PtSn(2.0 wt%)/MCM-41 were larger than that of PtSn(1.0 wt%)/MCM-41, indicating uniform distribution of metallic nanoparticles in the tin

modified catalysts. The average metal particle sizes over PtSnCe(0.5 wt%)/MCM-41, PtSnCe (1.0 wt%)/MCM-41 and PtSnCe (2.0 wt%)/MCM-41 catalysts were 2.5, 1.8 and 2.3 nm, respectively. The size distribution of metallic particles over PtSnCe (2.0 wt%)/MCM-41 and PtSnCe(0.5 wt%)/MCM-41 were larger than that of PtSnCe(1.0 wt%)/MCM-41, indicating a relatively uniform distribution of metallic nanoparticles in cerium modified catalyst. These results imply that suitable amount of Ce was favorable for the distribution of metallic particles, which was in good agreement with the measured results of chemisorption as given in **Table 5**.

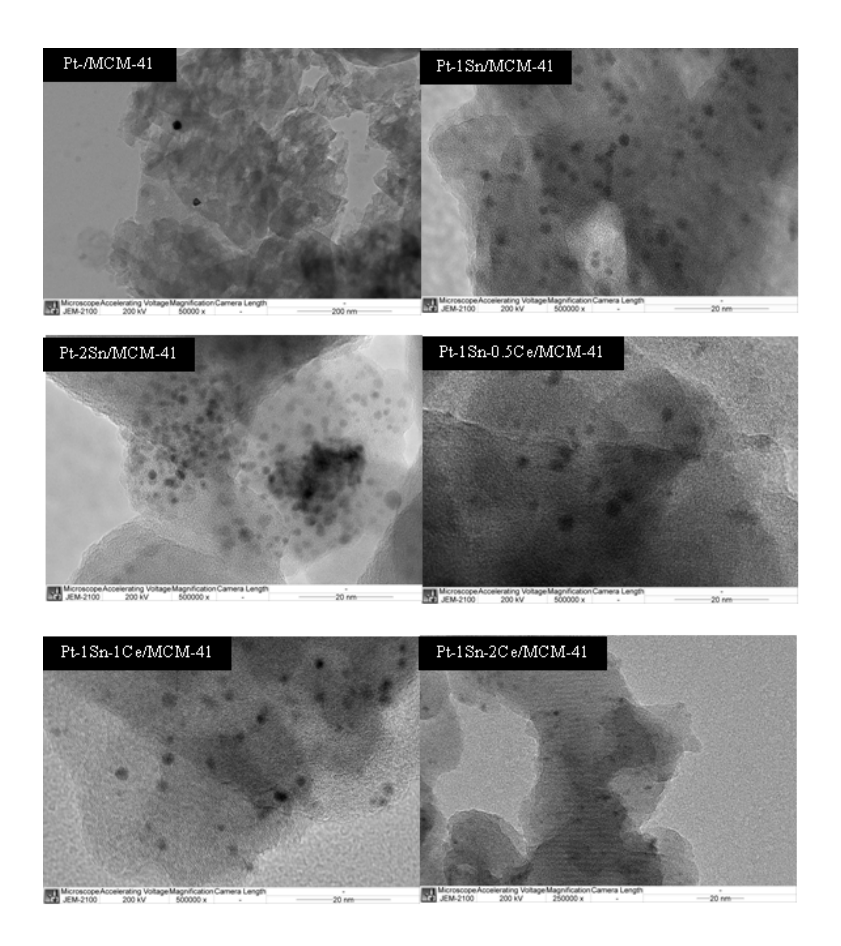


Figure 10 TEM micrographs of the Pt/MCM-41, Pt-Sn/MCM-41 and Pt-Sn-Ce/MCM-41catalysts

3.3.2 Catalytic performance

The catalytic performance in terms of propane conversion and propylene selectivity as a function of reaction time of Pt-Sn/MCM-41 and Pt-Sn-Ce/MCM-41 are plotted in **Figure 11**. It can be seen that all the catalysts showed activity decay with respect to reaction time, especially in the first hour. In the initial process of the reaction, the rate of coke formation over the catalyst was very fast. In this way, the catalyst deactivation was inevitable. This result is consistent with the increasing of propylene selectivity after the reaction time was prolonged. The results also showed that the Sn addition obvious improved the propane conversion and propylene selectivity. To explain this finding, it should be noted that on the bimetallic Pt-Sn catalysts, platinum was the only active metal and propylene was formed on the metal by dehydrogenation; the main cracking product (ethylene) was mainly formed from cracking on the carrier and the ethane was formed by hydrogenolysis of propane and by hydrogenation of ethylene, with both reactions taking place on the metal. Moreover, it can be seen from **Figure 11** that the addition of Sn also affect the propylene selectivity, for all the catalysts the reaction selectivity remained almost at about 87 % after the reaction.

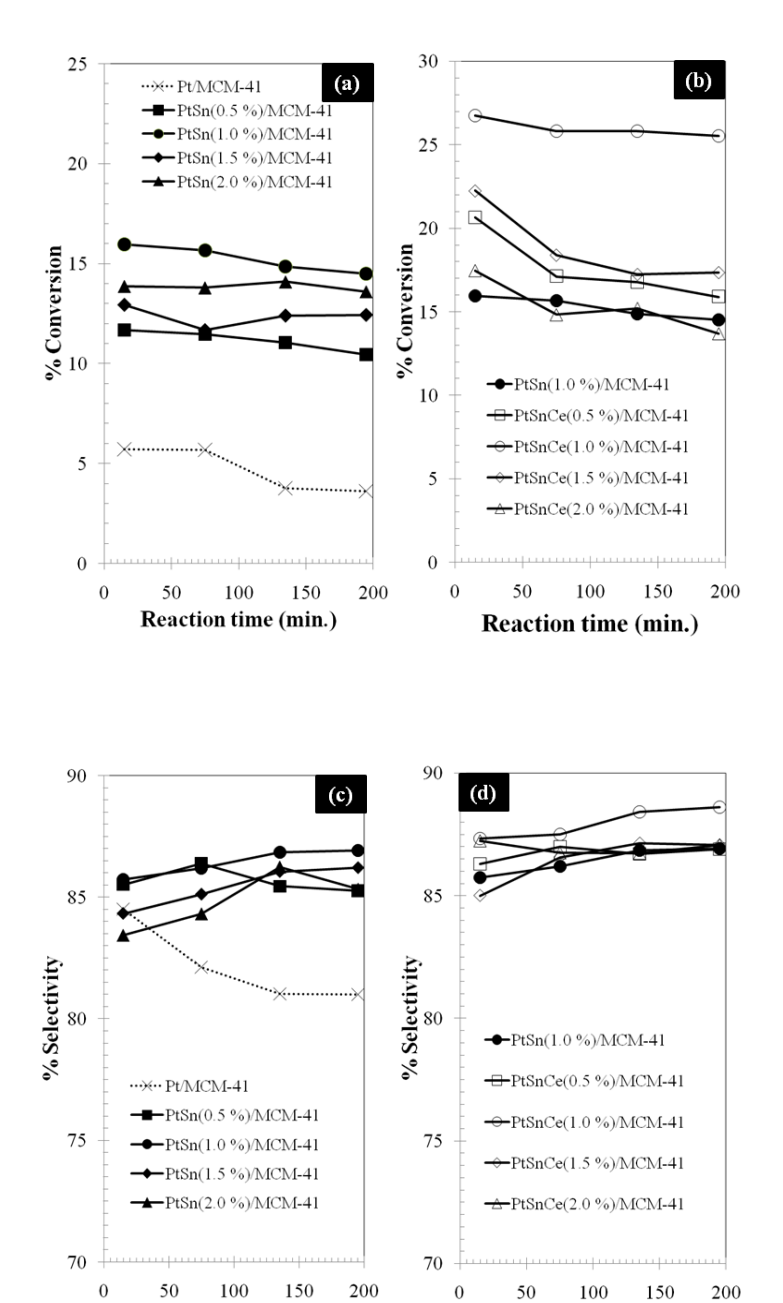


Figure 11 Plot between catalytic performance and reaction of all catalysts: (a) conversion vs reaction time of Pt-Sn/MCM-41 catalysts, (b) conversion vs reaction time of Pt-Sn-Ce/MCM-41 catalysts, (c) selectivity vs reaction time of Pt-Sn/MCM-41 catalysts and (d) selectivity vs reaction time of Pt-Sn/MCM-41 catalysts

Reaction time (min.)

Reaction time (min.)

The addition of Ce 0.5 wt% gave an obvious increase in the catalytic activity (initial conversion 18.67 %, and final conversion 12.90 %). Moreover, the conversion of propane increased with increasing amount of Ce from 0.5-1.0 wt%. The highest propane conversion was obtained on the catalyst promoted with Ce 1.0 wt%. These results indicated that the Ce promoter can make a significant impact on the catalytic performance of Pt-Sn/MCM-41 catalyst for propane dehydrogenation. However, with the excessive addition of Ce (1.5 - 2.0 wt%) the catalytic activity decreased. As analysis above, suitable addition of Ce to Pt-Sn/MCM-41 catalyst resulted in the increased the metallic dispersion. Moreover, in these cases, the presence of Ce can also change the interactions between Sn species and the support, which might improve the catalytic activity and stability of the catalyst. Figure 11 shows the propylene selectivity versus reaction time for the different catalysts. For all the catalysts, the selectivity to propylene increased gradually with the reaction time. Moreover, it can be seen from Figure 11 that the addition of Ce had little effect on the propylene selectivity and also reduced the deactivation. For all the catalysts the reaction selectivity remained at about 89 % after reaction time.

CHAPTER IV

Conclusions

The conclusions of these researches can divided in three parts.

4.1 Effect of promoters

The effect of dopants (Ce, K and Zn) on the physiochemical and catalytic properties of FSP-made Pt-Sn/Al₂O₃ was investigated in the dehydrogenation of propane. The resulting FSP-made catalysts consisted of single-crystalline particles exhibiting the characteristic of γ-alumina with average primary particle size of 7 to 9 nm. The Pt active sites increased after loading with Ce. On the other hand, the Pt active sites of Pt-Sn-Zn/Al₂O₃ and Pt-Sn-K/Al₂O₃ catalysts decreased dramatically after loading with K and Zn. Among the bi- and tri-metallic catalysts, Pt-Sn-Ce/Al₂O₃ exhibited the highest catalytic activity and selectivity in the dehydrogenation of propane. On the other hand, the catalytic activity and propene selectivity was decreased after loading with K and Zn. The better catalytic performance of the flame-made Pt-Sn-Ce/Al₂O₃ catalysts was correlated well to an increase of Pt metal active sites.

4.2 The effect of Ce loading content

The effect of Ce doping on the physiochemical and catalytic properties of FSPmade Pt and Pt-Sn/Al₂O₃ was investigated in the dehydrogenation of propane. The resulting FSP-made catalysts consisted of single-crystalline particles exhibiting the characteristic of γ -alumina with average primary particle size of 8 to 10 nm. The Pt active sites decreased after loading with Sn, whereas, the addition of Ce promoted the dispersion of Pt atoms. The lower amount of CO chemisorption on the Pt-Sn catalysts can be attributed to the formation of Pt-Sn ensembles or alloys that do not adsorb CO or the formation of an alumina matrix (i.e., in the form of Al-O groups) covering the Pt and Sn surfaces during FSP synthesis. While the improvement of Pt active sites could be explained by the inhibition of Pt cluster growth by addition of Ce atoms. Flame-made Pt-Ce/Al₂O₃ and Pt-Sn-Ce/Al₂O₃ catalysts, with cerium loadings in the range of 0.5–1.5 wt.%, exhibited a highly efficient performance for propane dehydrogenation to propylene. An optimum Ce loading that yielded the highest catalyst performance was determined to be ca. 1 wt%. Over Pt-Sn-1Ce/Al₂O₃ catalyst, we could get 56.5% of propane conversion and 95% propylene selectivity for the propane dehydrogenation reaction. Furthermore, Addition of Ce decreased the catalysts deactivation rates.

4.3 Effect of Ce addition on Pt-Sn/MCM-41 catalyst

In summary, the addition of Sn to Pt/MCM-41 catalyst has an obvious impact on the catalytic performance of propane dehydrogenation. When the amount of Sn was appropriate, the platinum dispersion increased obviously, while the percentage of deactivation decreased. Furthermore, TEM results demonstrate that the presence of Sn promoted the Pt/PtO particles distribution. When the appropriate amount of Ce was added in Pt-Sn(1.0 wt%)/MCM-41, the platinum dispersion increased explicitly which was in good agreement with the measured results of CO chemisorption and TEM. In these cases, it is suggested that the existence of Ce can strengthen the interaction between Sn species and the support, thereby larger amounts of tin can exist in oxidized form, which is advantageous to the reaction (agannesselfase). In our experiments, Pt-Sn-Ce(1.0 wt%)/MCM-41 catalyst exhibited the excellent performance of propane dehydrogenation, propane conversion above 25% and selectivity to propylene 89 % maintained during the 195 min reaction time.

Output ที่ได้จากโครงการ

งานวิจัยนี้ได้เริ่มดำเนินงานตั้งแต่ประมาณเดือน มิ.ย. 2553 สิ้นสุดโครงการ มิ.ย. 2556 รวมระยะเวลาดำเนินงาน 3 ปี ผลที่ได้รับจากงานวิจัย ได้แก่

- 1. สามารถสังเคราะห์ตัวเร่งปฏิกิริยาขนาดนาโนของแพลทินัม-ทิน-ซีเรียมที่อยู่บนตัว รองรับอะลูมินาและ MCM-41 ขึ้นได้ในขั้นตอนเดียวด้วยเทคนิคเฟลมสเปรย์ไพโรไลซิส และเคนิคเคลือบฝังแบบแห้งได้
- 2. การศึกษาการประยุกต์ใช้ตัวเร่งปฏิกิริยาดังกล่าวในปฏิกิริยาดีไฮโดรจิเนชันของโพรเพน พบว่าการเติมซีเรียมลงไปช่วยเพิ่มประสิทธิภาพของตัวเร่งปฏิกิริยาที่เตรียมขึ้นและมีสมบัติ ที่ดีกว่าตัวเร่งปฏิกิริยาที่เตรียมจากวิธีเดิมรวมถึงตัวเร่งปฏิกิริยาที่มีขายในท้องตลาด
- ได้เสนอผลงานเพื่อตีพิมพ์ในวารสารที่มี Peer review ระดับนานาชาติจำนวน 3 บทความ โดย 2 บทความได้รับการตีพิมพ์เรียบร้อยแล้ว และอีก 1 ผลงานกำลังอยู่ในระหว่างการเตรียม บทความ

ผลงานที่ได้รับการตีพิมพ์ในวารสารที่มี Peer review ระดับนานาชาติ

- S. Pisduangdaw, J. Panpranot, C. Chaisuk, K. Faungnawakij, O. Mekasuwandumrong "Flame Sprayed Tri-metallic Pt-Sn-X/Al₂O₃ Catalysts (X = Ce, Zn, and K) for Propane Dehydrogenation" Catalysis Communications, 12 (2011) 1161-1165.
- C. Chaisuk, P. Boonpitak, J. Panpranot, O. Mekasuwandumrong "Effects of Co dopants and flame conditions on the formation of Co/ZrO₂ nanoparticles by flame spray pyrolysis and their catalytic properties in CO hydrogenation" Catalysis Communications 12 (2011) 917–922.
- 3. **O. Mekasuwandumrong**, and J. Panpranot "Influence of Sn and Ce modification over Pt supported MCM-41 catalysts for propane hydrogenation" Catalysis Communications Prepared.

ภาคผนวก

- Reprint of the paper entitled "Flame Sprayed Tri-metallic Pt-Sn-X/Al₂O₃ Catalysts (X
 Ce, Zn, and K) for Propane Dehydrogenation" Catalysis Communications, 12
 (2011) 1161-1165.
- 2. Reprint of the paper entitled "Effects of Co dopants and flame conditions on the formation of Co/ZrO₂ nanoparticles by flame spray pyrolysis and their catalytic properties in CO hydrogenation" Catalysis Communications 12 (2011) 917–922.

Reference

- [1] M. M. Bhasin, J. H. McCain, B. V. Vora, T. Imai, P.R. Pujado, Appl.Catal. A: Gen., 221 (2001) 397.
- [2] Z. Nawaz, F. Wei, J. Ind. Eng. Chem. 17 (2011) 389.
- [3] S. B. Kogan, H. Schramm, M. Herskowitz, Applied Catalysis A: General 208 (2001) 185.
- [4] J. Salmones, J. Wang, J. A. Galicia, G. Aguilar-Rios, Journal of Molecular Catalysis A: Chemical 184 (2002) 203.
- [5] L. Bednarova, C. E. Lyman, E. Rytter, and A. Holmen, Journal of Catalysis 211 (2002) 335.
- [6] M. Larsson, M. Hultén, E. A. Blekkan, and B. Andersson, Journal of Catalysis 164 (1996) 44.
- [7] M. P. Lobera, C. Téllez, J. Herguido and M. Menéndez, Ind. Eng. Chem. Res. 47 (2008), 9314.
- [8] S. Pisduangdaw, J. Panpranot, C. Methastidsook, C. Chaisuk, K. Faungnawakij, P. Praserthdam, and O. Mekasuwandumrong, Applied Catalysis A: General 370 (2009) 1.
- [9] M. Larsson, B. Andersson, O.A. Bariås, A. Holmenc, Studies in Surface Science and Catalysis 88 (1994) 233.
- [10] O. A. Bariås, A. Holmen, and E. A. Blekkan, J. Catal. 158 (1996) 1.
- [11] Y. Zhang, Y. Zhou, A. Qiu, Y. Wang, Y. Xu and P. Wu, Catal.Commun., 7 (2006) 860.
- [12] A. Corma, A. Martinez, V. Martinez-Soria, J.B. Monton, J. Catal., 153 (1995) 25.
- [13] A. Corma, A. Martinez, V. Martinez-Soria, J. Catal., 169 (1997) 480.

- [14] A. Gurav, T. Kodas, T. Pluym, Y. Xiong, Aerosol Sci. Technol., 19 (1993) 411.
- [15] S.E. Pratsinis, S. Vemury, Powder Technol., 88 (1996) 267.
- [16] S. Alavi, B. Caussat, J.P. Couderc, J. Dexpert-Ghys, N. Joffin, D. Neumeyer, M. Verels, Advances in Sci. Technology A, 30 (2003) 417.
- [17] M. Piacentini, R. Strobel, M. Maciejewski, S. E. Pratsinis, A. Baiker, J. Catal., 243 (2006) 43.
- [18] R. Strobel, F. Krumeich, S. E. Pratsinis, A. Baiker, J. Catal., 243 (2006) 229.
- [19] M. J. Height, S. E. Pratsinis, O. Mekasuwandunrong, and P. Praserthdam, Appl. Catal. B, 63 (2006) 305.
- [20] R. Strobel, W. J. Stark, L. Madler, S. E. Pratsinis, and A. Baiker, J. Catal. 213 (2003) 296-304.
- [21] R. Strobel, F. Krumeich, W. J. Stark, S. E. Pratsinis, and A. Baiker, J. Catal. 222 (2004) 307-314.
- [22] S. Hannemann, J.-D.Grunwaldt, P. Lienemann, D. Gunther, F. Krumeich, S. E. Pratsinis, and A. Baiker, Appl. Catal. A: Gen., 316 (2007) 226-239.
- [23] S. Somboonthanakij, O. Mekasuwandumrong, J. Panpranot, T. Nimmanwudtipong, R. Strobel, S.E. Pratsinis, and P. Praserthdam, Catal. Lett. 119 (2007) 346-352.
- [24] S. Pisduangdaw, J. Panpranot, C. Methastidsook, C. Chaisuk, K. Faungnawakij, P. Praserthdam, O. Mekasuwandumrong Appl. Catal. A: Gen., 370 (2009) 1-6.
- [25] O. Mekasuwandumrong, S. Somboonthanakij, P. Praserthdam and J. Panpranot, Ind. Eng. Chem. Res. 48 (2009) 2819-2825.
- [26] C. Yu, H. Xu, Q. Ge, W. Li, J. Mol. Catal. A: Chem. 266 (2007) 80-87.
- [27] R. D. Cortright, J. A.Dumesic, J. Catal. 157 (1995) 576-583.

- [28] M. Tasbihi, F. Feyzi, M.A. Amlashi, A.Z. Abdullah, A.R. Mohamed, Fuel Process. Technol., 88 (2007) 883-889.
- [29] J. Silvestre-Albero*, J. Serrano-Ruiz, A. Sepu'lveda-Escribano and F. Rodrı'guez-Reinoso, Appl. Catal. A: Gen., 351 (2008) 16-23.
- [30] B.K. Vu, M.B. Song, I.Y. Ahn, Y.-W. Suh, D.J. Suh, W.-I. Kim, H.-L. Koh, Y.G. Choi, and E.W. Shin, Catalysis Today, Article in Press.
- [31] B.K. Vu, M.B. Song, I.Y. Ahn, Y.-W.Suh, D.J. Suh, W.-I. Kim, H.-L.Koh, Y.G. Choi, and E.W. Shin, Catal. Today, (2011) 214-220.
- [32] M. Merlen, P. Beccat, J.C. Bertolini, P. Delichere, N. Zanier, B. Didillon J. Catal., 159 (1996) 178–188.
- [33] H. Armendáriz, A. Guzmán, J.A. Toledo, M.E. Llanos, A. Vázquez, G. Aguilar-Ŕıos, Appl. Catal. A: Gen., 211 (2001) 69–80.
- [34] H. Lieske, J. Volter, J. Catal., 90 (1986) 96–105.
- [35] S. Damyanova, J.M.C. Bueno, Appl. Catal. A: Gen., 253 (2003) 135–150.
- [36] V. Pitchon, J.F. Zins, L. Hilaire, G. Maire, React. Kinet. Catal. Lett., 59 (2) (1996) 203–209.
- [37] B. K. Vu, M. B. Song, I. Y. Ahn, Y.-W. Suh, D. J. Suh, J. S. Kim, E. W. Shin, J. Ind. Eng. Chem. 17 (2011) 71-76.